



TITLE: Relation between crust development and heterocyclic aromatic amine formation when air-roasting a meat cylinder

AUTHORS: Alain Kondjoyan, Sylvie Chevolleau, Stéphane Portanguen, Jérôme Molina, Predrag Ikonic, Sylvie Clerjon, Laurent Debrauwer

This article is provided by author(s) and FINS Repository in accordance with publisher policies.

The correct citation is available in the FINS Repository record for this article.

NOTICE: This is the author's version of a work that was accepted for publication in *Food Chemistry*. Changes resulting from the publishing process, such as peer review, editing, corrections, structural formatting, and other quality control mechanisms may not be reflected in this document. Changes may have been made to this work since it was submitted for publication. A definitive version was subsequently published in *Food Chemistry*, Volume 213, December 2016, Pages 641–646. DOI: 10.1016/j.foodchem.2016.06.118

This item is made available to you under the Creative Commons Attribution-NonCommercial-NoDerivative Works – CC BY-NC-ND 3.0 Serbia



1

2 **Relation between crust development and heterocyclic aromatic amine**
3 **formation when air-roasting a meat cylinder**

4

5 Kondjoyan, Alain ^{1†}, Chevolleau, Sylvie ^{2,3}, Portanguen, Stéphane¹, Molina, Jérôme^{2,3}, Ikonic,
6 Predrag⁴, Clerjon, Sylvie¹, Debrauwer, Laurent ^{2,3}

7

8 ¹UR370 Qualité des Produits Animaux, INRA, F-63122 Saint Genès Champanelle, France.

9 ²INRA, UMR1331 TOXALIM, Research Center in Food Toxicology, MetaToul-AXIOM
10 Platform, F-31027 Toulouse, France.

11 ³Université de Toulouse, INPT, UPS, UMR1331, F-31062 Toulouse, France.

12 ⁴Institute of Food Technology, University of Novi Sad, Bulevar cara Lazara 1, 21000 Novi Sad,
13 Serbia.

14

15 **Abstract**

16 The meat crust that develops during cooking is desired by consumers for its
17 organoleptic properties, but it is also where heterocyclic aromatic amines (HAs) are
18 formed. Here we measured HAs formation during the development of a colored crust on
19 the surface of a beef meat piece. HAs formation was lower in the crust than previously
20 measured in meat slices subjected to the same air jet conditions. This difference is
21 explained by a lower average temperature in the colored crust than in the meat slices.
22 Temperature effects can also explain why colored crust failed to reproduce the
23 plateauing and decrease in HAs content observed in meat slices. We observed a
24 decrease in creatine content from the center of the meat piece to the crust area. In terms
25 of the implications for practice, specific heating conditions can be found to maintain a
26 roast beef meat aspect while dramatically reducing HAs content.

27

28 **Key words:** Crust, Heterocyclic amines, Heat, Juice, Transfer, Beef, Hot air.

29 **Highlights:**

30 HA formation and degradation differ between roast beef crust and meat slices;

31 Creatine content decreases from the center of the meat piece to the crust;

32 HA content can be dramatically reduced without losing a 'roasted' look.

[†] Corresponding author: UR370 Qualité des Produits Animaux, INRA, 63122 Saint-Genès-Champanelle, France, Tel: +33 (0)4 73 62 44 92 – Fax: +33 (0)4 73 62 40 89, email: alain.kondjoyan@inra.clermont.fr

33

34 **Abbreviations:**35 4,8-DiMeIQx: 2-amino-3,4,8-trimethyl-imidazo[4,5-*f*]quinoxaline36 AcONH₄: Ammonium acetate

37 ACN: Acetonitrile

38 AαC: 2-amino-9*H*-pyrido[2,3-*b*]indole39 DMIP: 2-amino-1,6-dimethylimidazo[4,5-*b*]pyridine

40 FDP: Freeze-Dried Product

41 Glu-P-1: 2-amino-6-methyldipyrido[1,2-*a*:3',2'-*d*]imidazole42 Glu-P-2: 2-aminodipyrido[1,2-*a*:3',2'-*d*]imidazole

43 HAs: Heterocyclic Aromatic Amines

44 IQ: 2-amino-3-methyl-imidazo[4,5-*f*]quinoline45 IQx: 2-amino-3-methyl-imidazo[4,5-*f*]quinoxaline

46 IR: Infrared

47 LD: *Longissimus dorsi*48 LL: *Longissimus lomborum*49 LT: *Longissimus thoracis*50 MeAαC: 2-amino-3-methyl-9*H*-pyrido[2,3-*b*]indole51 MeIQ: 2-amino-3,4-dimethyl-imidazo[4,5-*f*]quinoline52 MeIQx: 2-amino-3,8-dimethyl-imidazo[4,5-*f*]quinoxaline

53 MeOH: Methanol

54 MRM : Multiple Reaction Monitoring

55 PAH: Polycyclic Aromatic Hydrocarbons

56 PEEK: PolyEther Ether Ketone

57 PhIP: 2-amino-1-methyl-6-phenyl-imidazo-[4,5-*b*]pyridine58 SM: *Semimembranosus*59 TB: *Triceps brachei*60 TriMeIQx: 2-amino-3,4,7,8-tetramethyl-3*H*-imidazo[4,5-*f*]quinoxaline61 Trp-P-1: 3-amino-1,4-dimethyl-5*H*-pyrido[4,3-*b*]indole62 Trp-P-2: 3-amino-1-methyl-5*H*-pyrido[4,3-*b*]indole63 TSP-d₄: 3-(trimethylsilyl)-2,2',3,3'-tetradeuteropropionic acid

64

65

66

67

68 **1. Introduction**

69

70 Cooking meat forms trace amounts of heterocyclic aromatic amines (HAs). The effects
71 of HAs on human health have been widely investigated, and while the literature is not
72 unanimous on the associations between HAs and human cancers, their carcinogenic
73 effects have been proved on animals and on cell lines (Ollberding, Wilkens, Henderson,
74 Kolonel, & Le Marchand, 2012; Jamin et al., 2013). Moreover, even if the carcinogenic
75 risks of moderate consumption of well-done meat appear low (Nagao, 1999; Ollberding
76 et al., 2012), there are synergetic effects to consider. For example, a synergistic effect
77 has been identified with Polycyclic Aromatic Hydrocarbons (PAH) / PhIP mixtures on
78 cell lines, with an increase of the formation of DNA adducts derived from PhIP (Jamin
79 et al., 2013). Thus, understanding and reducing HAs formation during cooking remains
80 an important concern for consumer health.

81 HAs formation rate increases with temperature and depends on the time-temperature
82 history of the surface region, i.e. the “crust”, where HAs are formed. Crust development
83 also generates the specific roasted and grilled flavours and colour desired by consumers.

84 Several kinetic models of HAs formation and degradation have been developed in liquid
85 and meat juice systems (Arvidsson, Van Boekel, Skog, & Jägerstad, 1997; Arvidsson,
86 van Boekel, Skog, Solyakov, & Jägerstad, 1999) as well as in meat slices subjected to
87 jets of superheated steam or dry air in the 150-250°C temperature range (Kondjoyan et
88 al., 2010a, b). Concentrations of four of the studied HAs, i.e. IQx, MeIQx, 4,8-
89 DiMeIQx and PhIP, follows regular kinetic patterns. HAs degradation was studied in a
90 meat juice model system at 200 and 225 °C (Arvidsson et al., 1999). In meat slices,
91 HAs formation increases with treatment time and temperature during the first 10 min of
92 treatment (Kondjoyan et al., 2010a, b), after which HAs concentration either plateaus or
93 decreases at temperatures ≥ 200 °C. The increase in the formation of 4 HAs (MeIQx,

94 PhIP, norharman and harman) in function of the temperature and the cooking time has
95 also been shown recently by Gibis, Kruwinnus & Weiss (2015) in fried bacon.
96 Nevertheless, it is difficult to compare the concentrations of HAs because of the
97 differences in composition between the relatively lean beef and pork rather rich in fat.
98 No degradation was observed at 175 °C. At 200-250 °C, HAs degradation is dependent
99 on type of HAs and gas humidity. In our previous experiments in meat slices,
100 temperature was uniform throughout the meat, and the whole slice can be considered

101 'crust'. Moreover, the experiments were limited to 20 min. These parameters are key
102 factors when comparing HAs formation in liquid and solid media. However, the
103 situation is different during the development of a crust on the surface of a meat piece
104 during grilling or roasting. In these practical conditions, strong temperature and water
105 gradients the surface of the meat cut lead to crust formation and thickening.

106

107 Creatine and creatinine are known to be common precursors to the formation of all HAs
108 (Nagao, 1999; Bordas, Moyano, Puignou, & Galceran, 2004; Gibis & Weiss, 2010). For
109 example, half of the carbons of PhIP come from creatine and the other half from
110 phenylalanine (Zöchling & Murkovic, 2002). Creatine and creatinine also play a major
111 role the formation of IQx and its related derivatives (Borgen, Solyakov & Skog, 2001).
112 In meat, the concentration of creatine is about tenfold the concentration of creatinine.
113 Creatine dehydration occurs spontaneously and non-enzymatically in the muscle to
114 form creatinine (Purchas, Rutherford, Pearce, Vather & Wilkinson, 2004), but this
115 reaction is strongly promoted by increasing meat temperature (Mora, Sentandreu &
116 Toldra, 2008), which means cooking meat decreases creatine/creatinine ratio (Harris,
117 Lowe, Warnes & Orme, 1997; Mora et al., 2008). Model systems can be used to
118 modulate the reaction precursors to determine their effect on the formation of different
119 HAs, which cannot be done in meat pieces (Kondjoyan et al., 2010a, b; Bordas et al.,
120 2004; Arvidsson et al., 1997, 1999).

121

122 This paper aims at connecting HAs formation to the mechanisms which are responsible
123 for crust formation. A special device and procedure were used to accurately control a
124 thermal treatment mimicking the roasting of beef meat (Portanguen, Ikonic, Clerjon, &
125 Kondjoyan, 2014). Creatine content was also measured from the center of the meat
126 piece out to the area of crust formation to assess its potential correlation with the
127 formation of HAs such as PhIP or IQx. Specific heating conditions were also looked for
128 in order to maintain the roasted aspect on the surface of beef meat while reducing HAs
129 under a situation which mimics the baking of beef meat in a forced-convection oven.

130

131

132

133

134

135

136 **2. Materials and Methods**

137

138 **2.1. Sample preparations, heat treatments, and thickness measurements**

139

140 *Longissimus thoracis* muscles were taken from carcasses of 18-month-old heifers
141 immediately after slaughter. The muscles were cut into big pieces, aged for 12 days
142 under vacuum packed conditions, then frozen and stored at $-20\text{ }^{\circ}\text{C}$. Thermal Treatment
143 and temperature measurement were performed using: (1) an open jet system which
144 enables IR measurement of surface temperature, and (2) a specific device that partially
145 compensates for the heat shrinkage of the sample.

146

147 A cylinder of meat, 48 mm in diameter and 50–55 mm in height, was accurately cut
148 from big pieces of the previous muscles, following the procedure detailed in Kondjoyan
149 et al. (2010a, b). The meat cylinder was placed in a support formed by a bigger hollow
150 cylinder made in PEEK[®]. The cylindrical meat sample was pushed by a spring fixed to
151 a disc located at the bottom of the device onto a grid fixed by a lid at the top of the
152 device. Spring contraction was adjusted using four screws located under the disc. The
153 support was then placed under the center of an open jet system. During heat treatment,
154 air temperature at the outlet was either 160, 190, 225, or 260 $^{\circ}\text{C}$, and distance (d)
155 between sample surface and pipe outlet was set at 36 mm. Actual temperatures reached
156 on the surface of the meat sample are given in Table 1. Heating was stopped by sliding
157 the support beneath a $45\text{--}55\text{ m s}^{-1}$ jet flow of cold air (temperature $3\text{--}5\text{ }^{\circ}\text{C}$) produced
158 by a Ranque–Hilsch vortex tube. Meat surface temperature was measured continuously
159 throughout thermal treatment using a calibrated IR pyrometer (Kondjoyan et al. 2010a,
160 b). During heating and cooling, the temperatures of the air jet impacting the meat were
161 measured using a thermocouple fixed to the PEEK[®] cylinder and set 2 mm above the
162 meat surface. After cooling, the meat cylinder was removed from the support taking
163 every precaution not to tear away any crust while withdrawing the surface grid. Samples
164 were used to analyse crust thickness and HAs content.

165

166 To measure the thickness of the colored crust, the top of one half of the meat sample
167 was cut perpendicularly to the cylinder axis such that the thickness of the slice was
168 equal to the thickness of the brown-colored crust plus a further 2– 3 mm of “non-brown-

169 colored” crust. A set of pictures of crust area was taken using a camera ($\times 10$ zoom)
170 associated to binoculars ($\times 1.6$ or $\times 2$ magnification) and a $100 \times 0.1 = 10$ -mm scale
171 (PYSER-SGI, UK). The thickness of the colored area was measured visually from the
172 binocular images. Measurements were taken in at least five crust locations to obtain
173 repeatable average and standard deviation values. In a first step, GIMP2.6 software was
174 run on the image to accurately separate the brown-colored crust area from the non-
175 brown-colored area following the irregular border. In a second step, a calibration of
176 lengths was done using the pictures of the reference length taken in each image to avoid
177 any difference in image resolution. In a third step, average crust thickness and its
178 standard deviation were calculated from all the acquisitions obtained on different
179 portions of crust (specific programs developed using Matlab 7.0[®] and its image
180 processing toolbox).

181

182 *2.2. Quantification of creatine*

183

184 Creatine content was measured on meat cylinders exposed to the hot air jet at $192\text{ }^{\circ}\text{C}$ for
185 either 20 or 60 min. After the treatment, four 5 mm-thick slices of meat were cut from
186 the top of the cylinder perpendicularly to jet direction (Fig. 1, right). Creatine was
187 measured by NMR in raw and cooked meat samples. Microsamples (0.2 g) were ground
188 in $\text{Na}_2\text{HPO}_4/\text{NaH}_2\text{PO}_4 \cdot 12\text{H}_2\text{O}$ buffer at pH 5.0 (Acros Organics, Geel, Belgium). After
189 12 h of rest, the solution was filtered and centrifuged for 10 min at $14,500\text{ g}$ at room
190 temperature. Then, a 0.6 mL aliquot of the supernatant was then assayed by $^1\text{H-NMR}$
191 spectroscopy. Creatine was characterized by two characteristic resonance signals: a
192 singlet resonance at 3.03 ppm (CH_3) and a singlet resonance at 3.92 ppm (CH_2). The
193 integration of these two signals was proportional to the number of protons.
194 Quantifications were made with respect to a closed capillary containing TSP-d4 (3-
195 (trimethylsilyl)-2,2',3,3'-tetradeuteriopropionic acid, Sigma-Aldrich, Saint-Quentin-
196 Fallavier, France) measured relative to a 1.76 mmol.L^{-1} standard solution of creatine.

197

198 *2.3 Identification and quantification of HAs in the colored crust*

199

200 Thirteen different HAs (IQ, IQx, MeIQ, MeIQx, 4,8-DiMe-IQx, A α C, MeA α C, Trp-P-
201 1, Trp-P-2, PhIP, Glu-P1, Glu-P2, DMIP) were determined by UHPLC-APCI-MS/MS
202 based on an LC-APCI-MS/MS method developed for chicken meat (Chevolleau,

203 Touzet, Jamin, Tulliez & Debrauwer, 2007) and since adapted for analyzing beef meat
204 samples (Kondjoyan, et al., 2010a, b). Meat samples were treated as described in
205 previous papers (Kondjoyan, et al., 2010a, b).

206

207 Briefly, 1 g of lyophilized beef meat sampled from the whole cooked sample was first
208 treated with 1 M NaOH. The internal standard (TriMeIQx) was added at this stage at a
209 concentration of 50 pg/ μ L. After liquid/liquid extraction (methylene chloride, Extrelut),
210 purification by solid-phase extraction (Oasis MCX 60mg/3cc) and evaporation to
211 dryness, the resulting residue was re-dissolved in 200 μ L of the starting LC mobile
212 phase. Separation was performed on an Accela 600 LC system (Thermo Fisher
213 Scientific, Les Ulis, France), using a Hypersil GOLD C8 column (Thermo Fisher
214 Scientific, 50 x 2.1 mm, 1.9 μ m) with prefilter and a AcONH₄ (30 mM,
215 pH5/ACN/MeOH) gradient elution. 5 μ L of the final extract was injected, and
216 separation was performed at 30 °C at a flowrate of 0.5 mL/min. MS detection was
217 performed on a TSQ Vantage triple-stage quadrupole mass spectrometer (Thermo
218 Fisher Scientific) using positive APCI ionization based on two specific transitions for
219 each HA. Typical working parameters were as follows: discharge APCI current, 4 μ A;
220 nebulizer temperature, 420 °C; heated transfer capillary temperature, 250 °C; heated
221 transfer capillary voltage, 35 V; sheath gas flow rate, 40 a.u.; auxiliary gas flow rate, 8
222 a.u. The performance of the optimized method was characterized in terms of linearity (r^2
223 > 0.99 between 1 and 1000 pg/ μ L), repeatability of retention times (RSD=1.5–2.0%, n =
224 6) and area ratios (RSD =5–10%, n = 6), LoD 0.015-0.05 ng/g) and LoQ (0.05–0.2
225 ng/g). No matrix effect (checked by post-column addition of the 13 HAs mixture) was
226 observed. Each cooked meat sample was extracted and analyzed in triplicate. HA
227 contents were expressed in nanograms of compound per gram of freeze-dried product.

228

229 *2.4 Statistical analysis*

230

231 All results in Table 3 were analyzed for normal distribution and subjected to an analysis
232 of variance using HSD Tukey-test ($\alpha = 0.05$) using the STATISTICA 12 Software
233 (StatSoft France, France).

234

235

236

237

238 **3. Results and discussion**

239

240 **3.1. Variations in creatine content in the meat cylinder during heating**

241

242 In this study, results are expressed based on both dry matter (FDP) and as a function of
243 weight of the roasted product. Results expressed on a FDP basis made it possible to
244 track changes in creatine content regardless of juice loss variations. Results expressed
245 on a mass of cooked product basis made it possible to compare our results with the
246 literature. Figure 2 plots the profile of creatine content measured from the center of the
247 meat piece to its surface when the meat cylinder was subjected to a jet of hot air at
248 192 °C for 60 min. A 20 min treatment led to a similar profile shape but the contents
249 were different (*ca.* 20% less than in Figure 2; data not shown). At the center of the meat
250 piece, creatine concentration was 501 mg/100 g cooked meat (1.85 g/100 g FDP), which
251 matches to the concentration reported by Purchas, Busboom & Wilkinson (2006) for
252 raw meat (Table 2). Gibis et al. (2015) measured the creatine concentration in bacon at
253 different scales of time and temperature, the results show a decrease in creatine
254 concentration with increasing temperature. This is also observed in present study as a
255 function of depth in the meat, which is connected to the decrease of the temperature.
256 Concentration expressed as a function of FDP decreases steadily towards the meat
257 surface and then sharply once in the colored crust.

258

259 **3.2. HAs content in the colored crust**

260

261 U-HPLC-MS/MS was able to characterize and quantify 13 HAs with better
262 performances than achievable using classical LC-MS/MS. Four of these HAs, namely
263 Trp-P-1 Trp-P-2, A α C and MeA α C, were never detected in the coloured crust or only in
264 trace amounts, while Glu-P-1 and IQ was detected in quantities close to our LoQ in the
265 most drastic roasting conditions (210 °C, 90 min). Table 3 reports the concentrations of
266 the other HAs measured in the surface area (including the colored crust plus the small
267 portion of non-brown-colored area) of the meat cylinder.

268 The heat treatments can be divided into three categories according to HAs content. In
269 the first category (lines 1, 2, 4 and 5 in Table 3), jet temperature and heating duration
270 are less than or equal to 158 °C and 40 min, respectively. Only MeIQx and PhIP are

271 formed in more important quantities, with concentrations below 20 ng g⁻¹ FDP for
272 MeIQx and below 5 ng g⁻¹ FDP for PhIP. The second category concerns the longest
273 treatment at the lowest temperature (124 °C for 90 min) together with the shortest
274 treatment at 192 °C (lines 3 and 6, table 3). In this case, all the HAs are formed in
275 significant amounts except MeIQ and Glu-P-2. The MeIQx and PhIP concentrations
276 measured were 35–40 and 5–15 ng g⁻¹ FDP, respectively. In the third category, all the
277 HAs are formed in high amounts, except MeIQ which remained under 3 ng g⁻¹ FDP
278 (lines 7 to 11 in table 3). In this category, two major HAs reach concentrations up to
279 416 ng g⁻¹ FDP for MeIQx and to 255 ng g⁻¹ FDP for PhIP.

280 The effect of cooking time on HAs concentration was studied from results reported in
281 Table 3, using the HSD Tukey-test. Few effects of cooking time were not significant
282 (values highlighted in grey in Table 3), concerning in particular the formation of PhIP at
283 the lowest temperatures. Above 192 °C, time effect was found to be highly significant,
284 except for the specific cases of IQx at 20 and 40 min at a temperature of 210 °C. The
285 effect of time x temperature was also tested for the conditions corresponding to lines 1
286 to 3 and 9 to 11, showing shows a highly significant effect of the temperature (124 to
287 210 °C), of the cooking time (20, 40, 90 min) and of the two combined factors on the
288 formation of MeIQx and PhIP.

289

290 3.3. Discussion

291

292 The HAs concentrations measured in this study within the colored crusts of small roasts
293 can be compared to those measured in a thin slice of beef meat subjected to superheated
294 steam or dry air jets (Kondjoyan et al., 2010a, b). The MeIQx and IQx concentrations
295 within the colored crust of the small roasts were half the concentrations found in the
296 slices at identical jet temperature and treatment duration. The proportions were more
297 variable for the HAs known to form in a water activity-sensitive manner. The ratio of
298 amounts of HAs formed in the colored crust *versus* the slice ranged from 2.0 to 9.0 for
299 PhIP and from 0.8 to 2.0 for 4,8-DiMeIQx depending on the type of thermal treatment
300 (dry air or superheated steam). The lower HAs content found in colored crust developed
301 on the surface of the meat pieces compared to the thin slices can be attributed to either:
302 (1) local differences in precursor concentrations, (2) differences in the “reactivity” of
303 these precursors connected to the water activity in the food matrix, or (3) local
304 differences in in-product temperature.

305
306 The first explanation cannot be connected with an initial difference in HAs precursors in
307 the raw meat, as all the experiments were led on the same beef muscle, i.e. *Longissimus*
308 *thoracis*. Thus, the local variation in precursors content can only be attributed to
309 differences due to their migration over the course of the experiment. In this study,
310 creatine concentration decreased from 1.85 g/100 g FDP at the middle of the meat piece
311 to 0.7 in the 2.5 mm just under the cylinder surface when the meat cylinder was roasted
312 at 192 °C for 60 min. The literature (Table 2) reports that creatine concentration
313 decreases down to 310 mg/100 g during grilling (Purchas et al., 2006) and 178 mg/100
314 g during frying (Gibis & Weiss, 2010) where the creatine likely mainly undergoes
315 dehydration, leading to an increase of creatinine concentration. Initial creatinine content
316 in raw meat from *Longissimus thoracis* muscle ranges from 8.4 to 11.4 mg/100 g
317 (Kondjoyan et al., 2010b). If the increase of creatinine is proportional to the decrease in
318 creatine, then creatinine content in the crust would be multiplied by about 30-fold
319 compared to the initial raw meat content. This could have important ramifications for
320 the formation of HAs, especially PhIP, since Bordas et al. (2004) reported that a 25-fold
321 increase in creatinine doubled the PhIP concentration in a meat flavor model system
322 subjected to a dry treatment at 200 °C for 30 min, whereas there was almost no effect on
323 PhIP when the model system was subjected to wet treatment at 170 °C for 2 hours.
324 Moreover, during Bordas' experiments, creatine content was held constant while
325 creatinine content varied, whereas under our more realistic conditions, creatine and
326 creatinine contents varied in the opposite pattern. Thus, in our set-up, the relative effect
327 of creatine and creatinine content on HAs formation on the surface of a piece of meat
328 strongly heated and dried during crust formation remains open to debate, especially
329 since this effect of creati(ni)ne can be mixed with that of the amino-acids. Indeed,
330 Bordas et al. (2004) also observed a strong effect of variation in amino acids content on
331 PhIP formation whereas we did not measure amino acids content in the crust area here.

332
333 The second explanation based on difference on precursor reactivity is supported by the
334 fact that in previous studies, it was observed that despite a higher amount of precursors,
335 IQx, MeIQx and 4.8-DiMeIQx formed at lower rates in meat slices than in meat juice
336 (Arvidsson et al., 1999, Kondjoyan et al., 2010a, b).

337

338 However, the third explanation seems the most likely here, since thin slices can be
339 considered areas of high and homogeneous temperature whereas the colored crust
340 featured sharp temperature gradients resulting in a lower mean temperature in the crust
341 than in the slices. This difference stems directly from the development of the crust
342 structure on the surface of meat pieces. We previously showed that crust is a complex
343 structure displaying several distinct areas. The transition from non-crust to crust area
344 begins at the evaporation front (Portanguen et al., 2014). Just beyond this front, liquid is
345 replaced by vapour, but water content is still high. Therefore, water activity and
346 temperature remain close to 1.00 and 100 °C, respectively. Water content then decreases
347 toward the surface, which leads to areas of high-temperature gradients successively
348 dominated by the formation of colored Maillard compounds and of HAs, respectively.

349

350 This study quantified HAs inside the coloured crust. A schematic drawing of the
351 relative thickness of the different crust areas estimated after 70 minutes of treatment at
352 210 °C is given in Figure 3 (Portanguen et al., 2014). The area where the temperature is
353 greater than or equal to 200 °C is about 0.5 mm deep and thus represents less than one
354 third of the area where the in-product temperature is over 150 °C. This illustrates the
355 extent of the temperature gradients near the surface of the meat pieces, and also explains
356 why no plateau or decrease in HAs quantities were observed in the colored crust,
357 contrary to our previous studies on meat slices where HAs plateauing or degradation
358 were observed after just 10 minutes of heat treatment (Kondjoyan et al., 2010a, b). The
359 slow HAs degradation that could occur in the 200 °C area just under the crust surface is
360 likely overwhelmed by the strong HAs formation in the deeper area of the meat piece.

361

362 These observations tend to confirm that the major factor driving HAs formation and
363 degradation is time–temperature. However, water activity was also found to play an
364 important role during experiments on meat slices where HAs formation increased with
365 decreased water activity due to the use of dry-air jets instead of superheated steam jets
366 (Kondjoyan et al., 2010a, b). A better quantification of these different phenomena
367 would require accurate heat and mass transfer modelling since measures are delicate due
368 to the very thin areas which form the crust.

369

370 **3.4. Mitigation of consumer exposure to HAs**

371

372 During roasting, HAs concentrate in the upper part of the crust while other parts of the
373 meat piece do not get hot enough (i.e. below 124 °C) to start generating HAs. The effect
374 of time–temperature on HAs formation is clear in Table 3 showing that very low
375 amounts of MeIQx and PhIP only begin to form from 158 °C for 20 min. Indeed, the
376 quantities of MeIQx and PhIP measured at 158 °C for 20 min are approximately 35
377 times lower than the quantities measured at 158 °C for 40 min which, in turn, are still 3
378 to 10 times lower than at 192 °C for 20 min. The HAs concentrations expressed in Table
379 3 are per weight of crust based on FDP. Thus, crust mass also has to be factored in to
380 determine consumer exposure to HAs. We previously showed that the thickness of the
381 colored crust increases linearly with time (Portanguen et al., 2014). Note that Table 3
382 also gives the crust thicknesses measured after the different heat treatments. Crust
383 thicknesses greater than 3 mm were voluntarily discarded from analysis as not
384 representative of common cooking practices.

385

386 The air-jet heat treatment at 158 °C applied for 40 min leads to HAs contents that can be
387 considered very low in the thin colored crust. Thus, the real mass content of HAs can be
388 considered negligible even though the meat surface is visually perceived as ‘crust’. In
389 terms of practical implications, specific heating conditions can be found to maintain a
390 roast beef meat aspect while dramatically reducing HAs content in the meat. Moreover,
391 the fact that crust thickness increases linearly with time raises prospects for controlling
392 crust development during the roasting process. However, this thickness increase was
393 observed under specific air-jet situations and has yet to be confirmed for other cooking
394 conditions. More generally, the time-course evolution of surface and under-surface
395 temperatures depends on air-flow velocity and the heat exchanged by radiation, which
396 vary from one set of equipment to another. Thus, specific thermal studies are needed to
397 further determine and control the optimal conditions to ensure safe meat roasting for
398 different types of cooking equipments.

399

400 **4. Conclusion**

401

402 Less HAs form in colored crusts developing on the surface of meat pieces than in meat
403 slices subjected to the same time–temperature conditions. This can be explained
404 considering the temperature of the whole slice is very rapidly reaches to air temperature
405 whereas the crust features a sharp temperature gradient resulting in a net lower mean

406 temperature of the crust than the surrounding air. Temperature gradients can also
407 explain why even at the longest treatment times and highest jet temperatures, the
408 colored crust failed to reproduce the plateauing and decrease in HAs content observed
409 in meat slices (Kondjoyan et al., 2010a, b). A decrease of creatine (which may result in
410 an increase of creatinine) was measured from the center of the meat piece towards the
411 area of crust formation. This decrease was further promoted by increasing the
412 temperature, and could have impacted the formation of HAs, especially PhIP or IQx.
413 However, the analysis of the relative effects of the different precursors of HAs, and of
414 temperature and water activity in a complex media like meat would need more analysis
415 and would benefit from a transfer-reaction modelling approach (Kondjoyan et al.,
416 2014).

417

418 In terms of practical implications, we found specific heating conditions that maintain a
419 roast beef meat aspect while dramatically reducing HAs content in the meat subjected to
420 hot air jet conditions. However, further thermal studies will be needed to mitigate HAs
421 formation while maintaining the roast beef meat aspect considering different types of
422 cooking equipments. Sensory analysis will also be needed to analyse the impact of these
423 heating conditions on savour and flavour.

424

425

426

427

428

429

430

431

432

433

434

435

436

437

438

439

443

References

444

445 Arvidsson, P., Van Boekel, M.A. J.S., Skog, K., & Jägerstad, M. (1997). Kinetics of
446 formation of polar heterocyclic amines in a meat model system. *Journal of Food*
447 *Science*, 62(5), 911-916.

448 Arvidsson, P., van Boekel, M.A.J.S., Skog, K., Solyakov, A., & Jägerstad, M. (1999).
449 Formation of heterocyclic amines in a meat juice model system. *Journal of Food*
450 *Science*, 64(2), 216-221.

451 Bordas, M., Moyano, E., Puignou, L., & Galceran, M T. (2004). Formation and stability
452 of heterocyclic amines in a meat flavour model system. Effect of temperature,
453 time and precursors. *Journal of Chromatography. B Analytical Technologies in*
454 *the Biomedical and Life Sciences*, 802(1), 11-17.

455 Borgen, E., Solyakov, A., & Skog, K. (2001). Effect of precursor composition and
456 water on the formation of heterocyclic amines in meat model systems. *Food*
457 *Chemistry*, 74, 11-19.

458 Chevolleau, S., Touzet, C., Jamin, E., Tulliez, J., & Debrauwer, L. (2007). Dosage par
459 LC-APCI-MS/MS des amines aromatiques hétérocycliques formées lors de la
460 cuisson des viandes. *Science des Aliments*, 27(6), 381-396.

461 Gibis, M., & Weiss, J. (2010). Inhibitory effect of marinades with hibiscus extract on
462 formation of heterocyclic aromatic amines and sensory quality of fried beef
463 patties. *Meat Science*, 85(4), 735-742.

464 Gibis, M., Kruwinnus, M., & Weiss, J. (2015). Impact of different pan-frying conditions
465 on the formation of heterocyclic aromatic amines and sensory quality in fried
466 bacon. *Food Chemistry*, 168, 383-389.

467 Harris, R.C., Lowe, J.A., Warnes, K., & Orme, C.E. (1997). The concentration of
468 creatine in meat, offal and commercial dog food. *Research in Veterinary Science*,
469 62(1), 58-62.

470 Jamin, E.L., Riu, A., Douki, T., Debrauwer, L., Cravedi, J.P., Zalko, D., & Audebert,
471 M. (2013). Combined genotoxic effects of a polycyclic aromatic hydrocarbon
472 (B(a)P) and an heterocyclic amine (PhIP) in relation to colorectal carcinogenesis.
473 *PLoS One*, 8(3), e58591.

474 Kondjoyan, A., Chevolleau, S., Greve, E., Gatellier, P., Sante-Lhoutellier, V., Bruel, S.,
475 Touzet, C., Portanguen, S., & Debrauwer, L. (2010a). Formation of heterocyclic

- 476 amines in slices of *Longissimus thoracis* beef muscle subjected to jets of
477 superheated steam. *Food Chemistry*, 119(1), 19-26.
- 478 Kondjoyan, A., Chevolleau, S., Greve, E., Gatellier, P., Sante-Lhoutellier, V., Bruel, S.,
479 Touzet, C., Portanguen, S., & Debrauwer, L. (2010b). Modelling the formation of
480 heterocyclic amines in slices of *Longissimus thoracis* and *Semimembranosus* beef
481 muscles subjected to jets of hot air. *Food Chemistry*, 123(3), 659-668.
- 482 Kondjoyan, A., Kohler, A., Realini, C. E., Portanguen, S., Kowalski, R., Clerjon, S.,
483 Gatellier, P., Chevolleau, S., Bonny, J. M., & Debrauwer, L. (2014). Towards
484 models for the prediction of beef meat quality during cooking. *Meat Science*, 97,
485 323-331.
- 486 Mora, L., Sentandreu, M.A., & Toldra, F. (2008). Contents of creatine, creatinine and
487 carnosine in porcine muscles of different metabolic types. *Meat Science*, 79(4),
488 709-715.
- 489 Nagao, M. (1999). A new approach to risk estimation of food-borne carcinogens—
490 heterocyclic amines—based on molecular information. *Mutation*
491 *Research/Fundamental and Molecular Mechanisms of Mutagenesis*, 431(1), 3-12.
- 492 Ollberding, N.J., Wilkens, L.R., Henderson, B.E., Kolonel, L.N., & Le Marchand, L.
493 (2012). Meat consumption, heterocyclic amines and colorectal cancer risk: the
494 Multiethnic Cohort Study. *International Journal of Cancer*, 131(7), E1125-1133.
- 495 Polak, T., Andrenšek, S., Žlender, B., & Gašperlin, L. (2009). Effects of ageing and low
496 internal temperature of grilling on the formation of heterocyclic amines in beef
497 *Longissimus dorsi* muscle. *LWT - Food Science and Technology*, 42(1), 256-264.
- 498 Portanguen, S., Ikonic, P., Clerjon, S., & Kondjoyan, A. (2014). Mechanisms of crust
499 development at the surface of beef meat subjected to hot air: An experimental
500 study. *Food and Bioprocess Technology*, 7(11), 3308-3318.
- 501 Purchas, R.W., Rutherford, S.M., Pearce, P.D., Vather, R., & Wilkinson, B.H.P. (2004).
502 Cooking temperature effects on the forms of iron and levels of several other
503 compounds in beef *Semitenidosus* muscle. *Meat Science*, 68, 201-207.
- 504 Purchas, R.W., Busboom, J.R., & Wilkinson, B.H. (2006). Changes in the forms of iron
505 and in concentrations of taurine, carnosine, coenzyme Q (10), and creatine in beef
506 *Longissimus* muscle with cooking and simulated stomach and duodenal digestion.
507 *Meat Science*, 74(3), 443-449.

508 Zöchling, S., & Murkovic, M. (2002). Formation of the heterocyclic aromatic amine
509 PhIP: identification of precursors and intermediates. *Food Chemistry*, 79(1), 125-
510 134.
511
512

ACCEPTED MANUSCRIPT

513

Figure legends

514

515 **Figure 1:** Schematic representation of the sampling procedure for the measurement of
516 crust thickness, the quantification of HAs content, and the quantification of creatine in
517 five slices of meat.

518

519 **Figure 2:** Quantification of creatine at different depths in meat (subjected to a 192 °C
520 air jet during 60 min). Average creatine value in raw meat (1.9 g/100g FDP) is plotted
521 as a solid line. Dotted lines correspond to the standard deviation. For information
522 purposes, creatine concentrations are expressed both in g / 100 g FDP and in mg/100 g
523 cooked meat to facilitate comparison with literature data.

524

525 **Figure 3:** Schematic representation of the thickness of the different areas in the crust
526 after meat cylinder was subjected to the air jet heating at 210 °C for 70 min. These
527 thickness values are issues from the work of Portanguen et al. (2014).

528

529

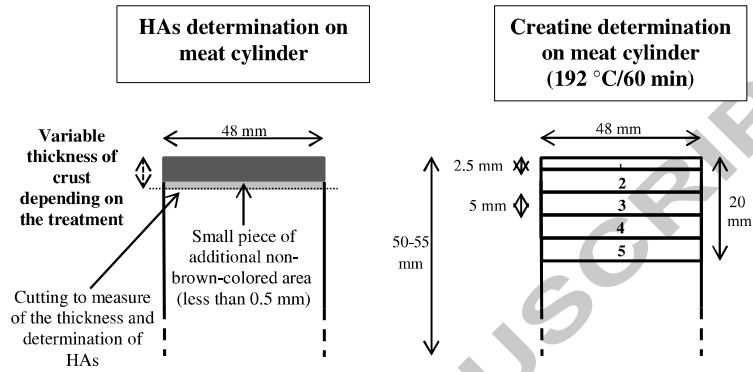
530

531

Figures

532

533



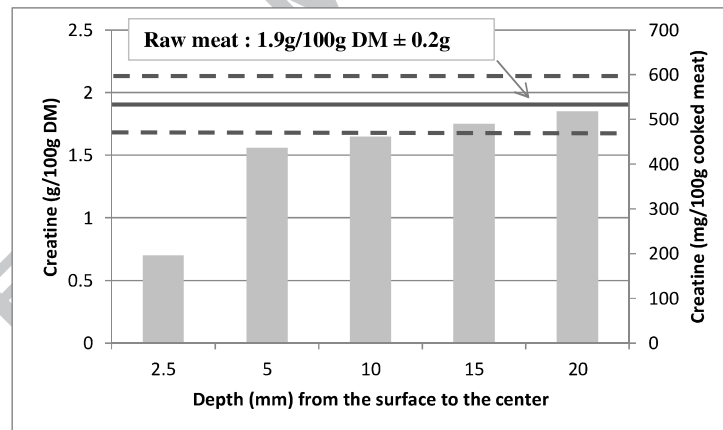
534

535

536 **Figure 1**

537

538



539

540

541 **Figure 2**

542

543

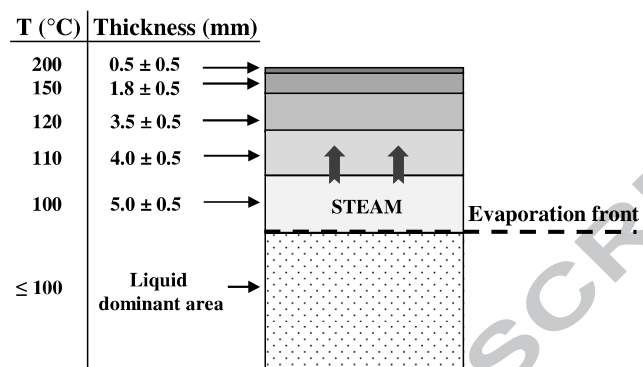
544

545

546

547

548



549

550

551 **Figure 3**

552

Table legends

Table 1: Heating times and temperatures corresponding to HAs measurements.

Table 2: Creatine and creatinine levels in beef depending on cooking conditions.

Table 3: Detailed formation of HA content in the developing meat crust (variation of crust thickness) given in nanograms of compound per gram of FDP (including the crust and the piece of additional non-brown-colored area). Values highlighted in grey: no significant effect of the cooking time on HA concentration. The line 5 gives the heating condition which maintain the roasted aspect meat while reducing HAs content in the meat.

* Crust too thick, not accepted by consumers.

Tables**Table 1**

T_{pipe} (°C)	T_{jet} (°C)	Cooking Time (min)
160	120 to 130	20, 40 and 90
190	150 to 160	20, 40
225	190 to 200	20, 30, 60 and 90
260	200 to 220	20, 40, 60 and 90

Table 2

Meat	Cooking method	Cooking temp. (°C)	Cooking time (min)	Creatine (mg/100g)	Creatinine (mg/100g)	Authors
Stewing-beef	Raw	/	/	364.5	7.8	Harris et al. (1997)
	Boiling	98	10-60	346.2-285.9	26.1-118.8	
Beef (ST)	Raw	/	/	401.0	5.8	Purchas et al. (2004)
Beef (TB)	Raw	/	/	329.0	5.6	Purchas et al. (2005)
Beef (LL)	Raw	/	/	383.5	6.1	Purchas et al. (2006)
	Grilling	71	/	310.6	43.2	
Beef (LD)	Raw	/	/	600.0	19.0	Polak et al. (2009)
Deep frozen beef patties (70g, 8 mm thick x 113 x 105 mm)	Raw	/	/	343.0*	9.9*	Gibis et al. (2010)
	Fried	230	2-3	226.9-178.5*	52.8-116.9*	
Beef (LT)	Raw	/	/	/	10.3	Kondjoyan et al. (2010b)
Beef (SM)	Raw	/	/	/	10.9	
Beef (LT)	Raw	/	/	470.7	/	Present study
	Baking	192	20	416.9	/	
		210	90	101.0	/	

*Levels based on dry matter.

Table 3

Lines	Roasting time (min)	Roasting Temp (°C)	Crust thickness (mm)	MeIQx (ng/g FDP)	IQx (ng/g FDP)	4,8-DiMeIQx (ng/g FDP)	PhIP (ng/g FDP)	MeIQ (ng/g FDP)	DMIP (ng/g FDP)	Glu-P-2 (ng/g FDP)
1	20	124	0.17	1.3 ±0.2	nd	nd	0.3 ±0.1	nd	nd	nd
2	40		0.19	19.4 ±0.6	1.7 ±0.2	nd	5.1 ±0.2	traces	nd	nd
3	90		0.42	41.1 ±7.0	2.3 ±0.1	2.2 ±0.1	5.8 ±0.7	traces	8.7 ±0.9	0.5
4	20	158	0.38	10.9 ±5.7	0.51	traces	3.6 ±1.4	traces	nd	nd
5	40		0.72	13.7 ±1.3	nd	traces	1.2 ±0.5	traces	2.9	trace
6	20	192	0.86	35.5 ±0.5	2.2 ±0.3	2.0 ±0.1	14.5 ±1.5	nd	6.3 ±0.7	traces
7	30		1.42	88.5 ±8.8	5.1 ±0.6	5.2 ±0.2	21.0 ±1.6	nd	13.1 ±1.9	traces
8	90		3.85	217.0 ±1.6	9.8 ±0.3	11.9 ±0.2	98.0 ±2.2	1.1 ±0.2	41.0 ±1.5	21.6 ±0.7
9	20	210	1.94	181.1 ±2.1	10.3 ±0.3	11.4 ±0.3	95.0 ±1.7	0.5 ±0.2	27.7 ±0.4	9.4 ±0.5
10	40		2.59	220.4 ±8.6	11.7 ±1.0	14.0 ±0.5	156.9 ±4.8	1.8 ±0.2	48.8 ±2.2	24.9 ±1.4
11*	90		5.82	417.0 ±14.8	21.6 ±1.0	26.9 ±0.9	255.9 ± 10.5	2.7 ±0.2	99.7 ±6.1	48.0 ±5.9